

FILE COPY

Naval Research Laboratory

Washington, DC 20375-5000



NRL Memorandum Report 6716

AD-A227 348

Dynamics of an Unsteady Diffusion Flame: Effects of Heat Release and Gravity

JANET L. ELLZEY* AND ELAINE S. ORAN**

**Berkeley Research Associates
Springfield, VA*

***Laboratory for Computational Physics and Fluid Dynamics Division*

September 27, 1990



Approved for public release; distribution unlimited.

90 10 04 068

| REPORT DOCUMENTATION PAGE | | | Form Approved OMB No. 0704-0188 | |
|---|---|--|---|---|
| Public reporting burden for this collection of information is estimated to average 1 hour per response, including the time for reviewing instructions, searching existing data sources, gathering and maintaining the data needed, and completing and reviewing the collection of information. Send comments regarding this burden estimate or any other aspect of this collection of information, including suggestions for reducing this burden, to Washington Headquarters Services, Directorate for Information Operations and Reports, 1215 Jefferson Davis Highway, Suite 1204, Arlington, VA 22202-4302, and to the Office of Management and Budget, Paperwork Reduction Project (0704-0188), Washington, DC 20503. | | | | |
| 1. AGENCY USE ONLY (Leave blank) | | 2. REPORT DATE 1990 September 27 | | 3. REPORT TYPE AND DATES COVERED Continued |
| 4. TITLE AND SUBTITLE Dynamics of an Unsteady Diffusion Flame: Effects of Heat Release and Gravity | | | 5. FUNDING NUMBERS PE - 61153N PR - DN280-071 TA - RR-011-0943 WU - 44-153000 | |
| 6. AUTHOR(S) Janet L. Ellzey* and Elaine S. Oran | | | | |
| 7. PERFORMING ORGANIZATION NAME(S) AND ADDRESS(ES) Naval Research Laboratory Washington, DC 20375-5000 | | | 8. PERFORMING ORGANIZATION REPORT NUMBER NRL Memorandum Report 6716 | |
| 9. SPONSORING/MONITORING AGENCY NAME(S) AND ADDRESS(ES) Office of Naval Research 800 N. Quincy Street Arlington, VA 22217-5000 | | | 10. SPONSORING/MONITORING AGENCY REPORT NUMBER | |
| 11. SUPPLEMENTARY NOTES *Berkeley Research Associates, Springfield VA | | | | |
| 12a. DISTRIBUTION / AVAILABILITY STATEMENT Approved for public release; distribution unlimited. | | | 12b. DISTRIBUTION CODE | |
| 13. ABSTRACT (Maximum 200 words) This report presents time-dependent axisymmetric numerical simulations of an unsteady diffusion flame formed between a $H_2 - N_2$ jet and a coflowing air stream. The computations include the effects of convection, molecular diffusion, thermal conduction, viscosity, gravitational forces, and chemical reactions with energy release. Previous work has shown that viscous effects are important in these flames and, therefore, all of the viscous terms in the compressible Navier-Stokes equations are included. In addition, the resolution is increased so that the large, vortical structures in the coflowing gas are resolved and the boundary conditions are improved so that the velocity field near the jet is more realistic. Computations with and without chemical reactions and heat release, and with and without gravity, are compared. Gravitational effects are insignificant in the nonreacting jet but in the reacting jet gravity produced the relatively low-frequency instabilities typically associated with flame flicker. Kelvin-Helmholtz instabilities develop in the region between the high-velocity and low-velocity fluid when there are no chemical reactions, but heat release dampens these instabilities to produce a mixing region which is almost steady in time. | | | | |
| 14. SUBJECT TERMS Unsteady diffusion flame Heat release and gravity | | | 15. NUMBER OF PAGES 20 | |
| | | | 16. PRICE CODE | |
| 17. SECURITY CLASSIFICATION OF REPORT UNCLASSIFIED | 18. SECURITY CLASSIFICATION OF THIS PAGE UNCLASSIFIED | 19. SECURITY CLASSIFICATION OF ABSTRACT UNCLASSIFIED | 20. LIMITATION OF ABSTRACT UL | |

CONTENTS

| | |
|--|---|
| INTRODUCTION | 1 |
| NUMERICAL METHOD | 2 |
| APPLICATION TO UNSTEADY DIFFUSION FLAMES | 4 |
| RESULTS | 5 |
| Nonreacting Jet | 5 |
| Reacting Jet | 5 |
| DISCUSSION AND CONCLUSIONS | 6 |
| ACKNOWLEDGMENTS | 7 |
| REFERENCES | 8 |

| | |
|----------------------|-------------------------------------|
| Accession For | |
| NTIS GRA&I | <input checked="" type="checkbox"/> |
| DTIC TAB | <input type="checkbox"/> |
| Unannounced | <input type="checkbox"/> |
| Justification | |
| By | |
| Distribution/ | |
| Availability Codes | |
| Dist | Avail and/or Special |
| A-1 | |



DYNAMICS OF AN UNSTEADY DIFFUSION FLAME: EFFECTS OF HEAT RELEASE AND GRAVITY

INTRODUCTION

Experiments on laminar diffusion flames have shown that gravity affects the flame length and width as well as its extinction characteristics (1-4). These studies have been conducted in drop towers and have focused on fuel jets with very low velocities of less than 50 cm/s. Although these experiments have increased our basic understanding of laminar diffusion flames by emphasizing the importance of buoyancy, it is not clear how to apply these results to higher-velocity flames which are unsteady or fluctuating. Studying higher-velocity fuel jets from larger nozzles is more difficult experimentally because the flames can be quite long and the instabilities may not have time to evolve during a single experiment. Through numerical simulations, we can examine an unsteady flame with and without gravity in the kind of detail that is not practical in an experiment.

Two types of instabilities are observed in low-speed diffusion flames (5,6). The high-frequency structures grow from Kelvin-Helmholtz instabilities at the interface between the high-velocity and low-velocity fluid and typically have frequencies of a few hundred Hertz. The low-frequency structures form in the region outside the flame zone with typical frequencies of 10-20 Hertz.

This paper examines the effect of heat release and gravity on the formation and evolution of these two types of instabilities by presenting a series of time-dependent, two-dimensional simulations of an axisymmetric H_2-N_2 jet in a coflowing air stream. The calculations include convection, thermal conduction, molecular diffusion, viscosity, chemical reactions with energy release, and gravitational forces. This model is based on the one developed by Laskey (7), which includes a new algorithm for convective transport developed by Patnaik et al. (8). Previously, Laskey (9) presented computations of diffusion flames of the type presented here and Patnaik et al. (10) used a similar model to study the stability properties of very low-speed premixed flames. All of these efforts have tested the various parts of the model and have given credibility to its overall validity.

These computations are different from previous ones reported by Laskey et al. (9) and Ellzey et al. (11) for several reasons. Greater resolution and improved boundary conditions now allow correct zero-gravity computations. The energy-release model now properly limits the final temperatures allowed and no longer produces a strong recirculation zone at the jet exit. Viscosity has been shown to be very important in diffusion flames at these velocities (11) and is, therefore, included in all of the calculations presented in this paper.

NUMERICAL METHOD

The numerical model consists of separate algorithms for the various processes, and these algorithms are coupled by timestep splitting methods. Table I is an outline of one computational timestep. Given a set of initial values for the basic variables, an appropriate computational timestep is estimated based on accuracy and stability criteria. Then the effects of thermal conduction are evaluated using a two-dimensional explicit finite-difference model (7). Thermal conductivities, for the individual species were calculated from kinetic theory over the temperature range 300 to 3300 K, these values were fit to a third-order polynomial, and then are used to calculate the mixture thermal conductivity (13). Molecular diffusion is included using an explicit finite-difference formulation. First, the diffusion velocities are calculated according to Fick's law and then corrected (13) to satisfy the requirement that the sum of the diffusion fluxes is zero. Binary diffusion coefficients, calculated from kinetic theory (14), are used to compute the diffusion coefficients for a particular species in a mixture (13). The viscosity coefficients μ_k , calculated from kinetic theory over the temperature range 300 to 3000K and fit to a third order polynomial, were used to compute the mixture viscosity (15). The model for chemical reactions and heat release is an extension of the Parametric Diffusion Reaction Model (7,12), which is designed to replace the integration of the full, detailed set of ordinary differential equations representing the chemical kinetics. A single, global reaction is used but the reaction is not instantaneous. Instead, the finite reaction rate is

Table I. One Timestep in the Diffusion-Flame Model

| | |
|--------------------------------|--|
| Given Initial Variables | |
| 1. Determine Timestep | |
| 2. Thermal Conduction | |
| | Integrate from t to $t + \Delta t$: |
| | Calculate $\Delta\epsilon_1$. Do not update any variables. Subcycle as necessary. |
| 3. Ordinary Diffusion | |
| | Integrate from t to $t + \Delta t$: |
| | Only update $\{n_i(x)\}$. Calculate $\Delta\epsilon_2$. Subcycle as necessary. |
| 4. Viscosity | |
| | Integrate from t to $t + \Delta t$: |
| | Only update $\rho\vec{v}$. Calculate $\Delta\epsilon_3$. |
| 5. Chemical Reactions | |
| | Integrate from t to $t + \Delta t$: |
| | Only update $\{n_i(x)\}$. Calculate $\Delta\epsilon_4$. |
| 6. Convective Transport | |
| | Integrate from t to $t + \Delta t$: |
| | x direction transport, then update $\rho, \rho\vec{v}, E, n_i$. |
| | y direction transport, then update $\rho, \rho\vec{v}, E, n_i$. |
| | Implicit correction, then update p, ϵ , and E . |
| 7. Increment Time and go to 1. | |

determined such that the maximum temperature in a one-dimensional transient diffusion flame is the adiabatic flame temperature for a stoichiometric mixture of the fuel and oxidizer. The transport of density, momentum, energy, and individual species density is accomplished through the high-order implicit method, BIC-FCT (8). This involves an explicit step, based on the standard FCT algorithm (16), and then an implicit correction.

The general timestep splitting approach for coupling the various physical processes was developed for slow-flow implicit calculations. In these computations, the change in internal energy resulting from each individual process is not incorporated into the solution as soon as it is computed, but instead is accumulated, as indicated by the $\{\epsilon_i\}$ in Table 1. The entire change in internal energy is then added to the

energy equation in the fluid convection step 6. The coupling technique has been described by Oran and Boris (16), and a modification by Patnaik et al. (17) has been shown to allow for a greater addition of energy per timestep while maintaining numerical stability.

In essence, the model solves the time-dependent two-dimensional conservation equations for mass density, ρ , momentum, $\rho\mathbf{v}$, and total energy, E and these are coupled to models for chemical reactions among the species $\{n_i\}$ with subsequent heat release, molecular diffusion, thermal conduction, viscosity, and gravitational forces. Additional equations include the perfect gas equation of state and a relation between the internal energy and the pressure. The specific set of equations and more detailed discussions of the numerical methods are given in References (7) and (12).

The computations described in this paper, using the enlarged computational grid and including all of the physical processes, require 0.7 s/computational timestep on a Cray YMP. This means that a typical calculation, about 50,000 timesteps, requires about 10 hours of computer time.

APPLICATION TO UNSTEADY DIFFUSION FLAMES

The computational grid for the region near the jet and the initial conditions are shown in Figure 1. The full domain is 10 cm \times 172 cm and consists of 128 \times 224 cells. Cells of approximately 0.02 cm are concentrated around the jet exit. Beginning at $r = 1$ cm, the size of each cell is increased by 3% over the size of its neighboring cell for all simulations. The cells in the axial direction for all simulations are stretched by 3% starting at $z = 1$ cm. A fuel mixture consisting of 78% H_2 and 22% N_2 by volume flows through a jet of radius 0.5 cm at 10 m/s at the lower boundary. Air flows through the outer annular region between $r = 0.5$ and $r = 10.0$ cm at 30 cm/s. The outer boundary at $r = 10.0$ cm is a free-slip wall. The inner boundary at $r = 0.0$ is the jet centerline. An outflow boundary is specified at $z = 172$ cm where the pressure is adjusted to atmospheric.

RESULTS

Nonreacting Jet

Figure 2 shows the instantaneous contours of axial and radial velocity and mole fraction late in the simulation of zero-gravity nonreacting jet. Kelvin-Helmholtz instabilities occur near the jet exit leading to vortical structures that then convect downstream. These structures, which transport fuel and oxidizer radially and broaden the mixing zone, weaken substantially in the first ten jet diameters. Small radial velocities, not evident in the contours, still exist at this point. Figure 3 shows the mean and rms velocity for the nonreacting jet at three axial locations. At $z = 0.5$ cm, the mixing region is narrow with only small fluctuations of a few cm/s. At $z = 1.0$ cm, the instabilities result in large fluctuations across the entire jet core. By $z = 10$ cm, there are small fluctuations across the entire jet region. The results for the nonreacting jet with gravity are not distinguishable from those for the same jet in zero gravity, and so are not shown here.

Reacting Jet

Instantaneous contours late in the calculation of the reacting jet in zero gravity, Figure 4, show that the volumetric expansion and the change in temperature have a significant effect on the flow. The radial velocities arise from the expansion at the flame front but are relatively uniform. The axial velocity and concentration fields are steady in time. Figure 5, the mean and rms velocity for this case, show that the mixing region is wider due to the expansion. Fluctuations are insignificant and not visible on the plot.

Figure 6 shows that gravity changes the flow significantly. Instabilities form outside the reaction zone in the region with large temperature and density gradients. The maximum radial velocity is approximately 30 cm/s and occurs at the center of the structure. The concentration and temperature fields are distorted as these instabilities convect downstream. The flame front lies at the fuel-oxidizer interface in the region of maximum temperature and fluctuates in time. Figure 7 shows a

time sequence of the H_2O mole-fraction contours. In the first frame, a bulge is developing on the outside of the H_2O contours. In subsequent frames, it rolls up and moves downstream. In the final frame, it is moving out of the domain shown as the next instability forms below it. These outer, slower-moving vortical structures occur at approximately 15 Hz.

DISCUSSION AND CONCLUSIONS

Comparisons of the four computations of the 10 m/s $H_2 - N_2$ jet into the 30 cm/s coflowing air background shows that gravity and heat release interact substantially to change the flow. Without chemical reactions and subsequent heat release, gravity does not noticeably change the velocity or concentration fields. Even though there are significant density gradients between the $H_2 - N_2$ fuel jet and the co-flowing air, these gradients occur in a region of relatively high velocity where momentum effects dominate.

In the reacting jet, there are significant density gradients in the coflow region where the velocity is low. These gradients are due to the conduction of heat away from the reaction zone. In this region, the bouyant forces dominate and large instabilities form. These have been observed in experiments for many years (6, 18-20) and are considered to be responsible for flame flicker.

Volumetric expansion and the effects of changing temperature stabilize the mixing region of the reacting jet. The increase in viscosity with temperature accounts for part of the stabilization but analytical results show that inviscid instabilities are also damped by heat release (21). Preliminary computations with constant viscosity indicate that the stabilization effect due to the change in viscosity with temperature may be insignificant compared to the effect of heat release. Previous calculations (11) show that even without including viscosity, heat release reduces the strength of the Kelvin-Helmholtz instability.

Future computations are proceeding in several different directions. First, we are considering the downward-propagating diffusion flame and how this differs from

upward and zero-gravity flames. Second, we are including the coflow velocity so that the computations have the same parameters as recent experiments at the Air Force Wright Aeronautical Laboratory. At that point, detailed comparisons will be made between the computations and experimental results. We are continuing to develop the energy-release model so that the energy release as a function of temperature is better represented. Finally, we have been investigating new types of computers that might allow full-chemistry or three-dimensional computations of such flames.

ACKNOWLEDGMENTS

This work was sponsored by the Naval Research Laboratory through the Office of Naval Research. We thank Dr. W.M. Roquemore from the Air Force Wright Aeronautical Laboratory for his support and suggestions. This work is based on an earlier computer code, Axisymmetric, Low-speed Jet Flame (ALJF) code, written by Dr. Kenneth Laskey. In addition, the authors would like to acknowledge the help and advice of Drs. Gopal Patnaik and Kenneth Laskey. The computations were performed at the NAS computer facility at NASA Ames Research Center.

REFERENCES

1. Cochrane, T.H. and Mascia, W.J., "Effects of Gravity on Laminar Gas Jet Diffusion Flames," NASA TN D-5872, June, 1970.
2. Cochrane, T.H. and Mascia, W.J., Proceedings of *Thirteenth Symposium (International) on Combustion*, pp. 821-829, The Combustion Institute, Pittsburgh, PA, 1970.
3. Haggard, J.B. and Cochrane, T.H., *Combust. Sci. Tech.*, 5, 291-298, 1972.
4. Haggard, J.B. and Cochrane, T.H., "Hydrogen and Hydrocarbon Diffusion Flames in a Weightless Environment," NASA TN D-7165, February, 1972.
5. Yule, A.J., Chigier, N.A., Ralph, S., Boulderstone, R., and Ventura, J., *AIAA J.*, 19, 752-760, 1981.
6. Chen, L.D., Seaba, J.P., Roquerore, W.M., and Goss, L.P., *Twenty-Second Symposium (International) on Combustion*, 677-684, The Combustion Institute, Pittsburgh, PA, 1988.
7. Laskey, K. J., *Numerical Study of Diffusion and Premixed Jet Flames*, Ph.D. dissertation, Department of Mechanical Engineering, Carnegie-Melon University, Pittsburgh, PA, 1988.
8. Patnaik, G., Boris, J.P., Guirguis, R.H., and Oran, E.S., *J. Comput. Phys.*, 71, 1-20, 1987.
9. Laskey, K.J., Ellzey, J.L., and Oran, E.S., "A Numerical Study of an Unsteady Diffusion Flame," AIAA Paper 89-0572, AIAA, Washington, DC, 1989.
10. Patnaik, G., Kailasanath, K., Laskey, K.J., and Oran, E.S., *Twenty-Second Symposium (International) on Combustion*, 1517-1526, The Combustion Institute, Pittsburgh, PA, 1988.
11. Ellzey, J.L., Laskey, K.J., and Oran, E.S., "Dynamics of an Unsteady Diffusion Flame: Effects of Heat Release and Viscosity," accepted by *AIAA Progress in Astronautics and Aeronautics*, 1989.
12. Ellzey, J.L., Laskey, K.J., and Oran, E.S., "A Study of Confined Diffusion

- Flames," submitted to *Combust. Flame*, 1989.
13. Kee, R.J., Dixon-Lewis, G., Warnatz, J., Coltrin, M.E., and Miller, J.A., *A Fortran Computer Code Package for the Evaluation of Gas-Phase Multicomponent Transport Properties*, SAND86-8246, Sandia National Laboratory, 1986.
 14. Kailasanath, K., Oran, E.S., and Boris, J.P., *A One-Dimensional Time-Dependent Model for Flame Initiation, Propagation, and Quenching*, NRL Memorandum Report 4910, Naval Research Laboratory, Washington, DC, 1982.
 15. Wilke, C.R., *J. Chem. Phys.*, 18, 578-579, 1950.
 16. Oran, E.S., Boris, J.P., *Numerical Simulation of Reactive Flow*, Elsevier, New York, 1987.
 17. Patnaik, G., Laskey, K.J., Kailasanath, K., Oran, E.S., and Brun, T.A., *FLIC - A Detailed, Two-Dimensional Flame Model*, NRL Memorandum Report 6555, Naval Research Laboratory, Washington, DC, 1989.
 18. Chamberlin, D.S., and Rose, A., *First Symposium on Combustion*, p. 27, The Combustion Institute, Pittsburgh PA, 1965.
 19. Kimura, I., *Tenth Symposium (International) on Combustion*, p. 1295, The Combustion Institute, Pittsburgh, PA, 1965.
 20. Ballantine, A. and Bray, K.N.C., *Sixteenth Symposium (International) on Combustion*, p. 777, The Combustion Institute, Pittsburgh, PA, 1977.
 21. Mahalingam, S., Cantwell, B., and Ferziger, J., "Effects of Heat Release on the Structure and Stability of a Coflowing, Chemically Reacting Jet," AIAA Paper 89-0661, AIAA, Washington, DC, 1989.

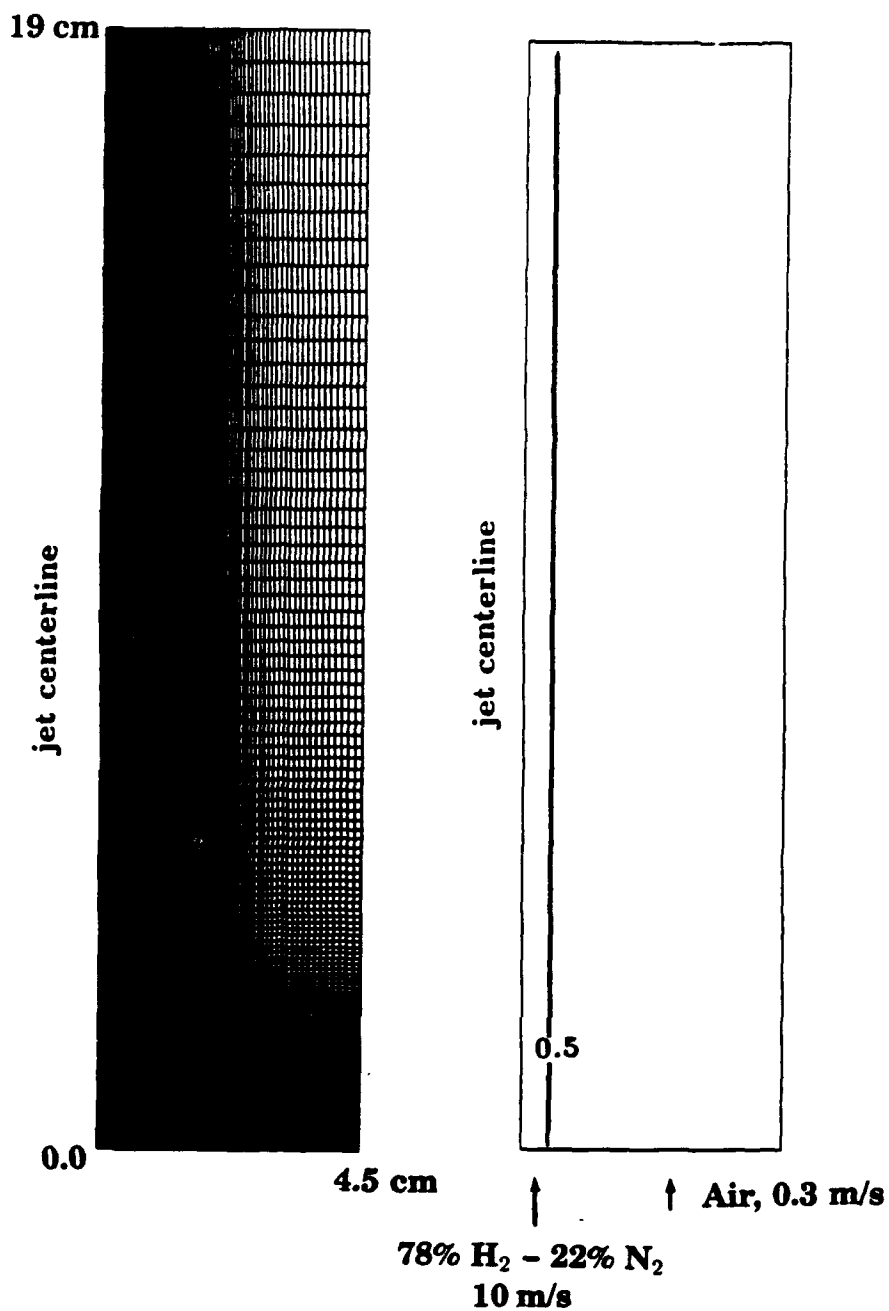


Figure 1. Computational domain and initial conditions for the computations of a $H_2 - N_2$ jet into coflowing air. Note that the figures only show the part of the full domain with the high resolution.

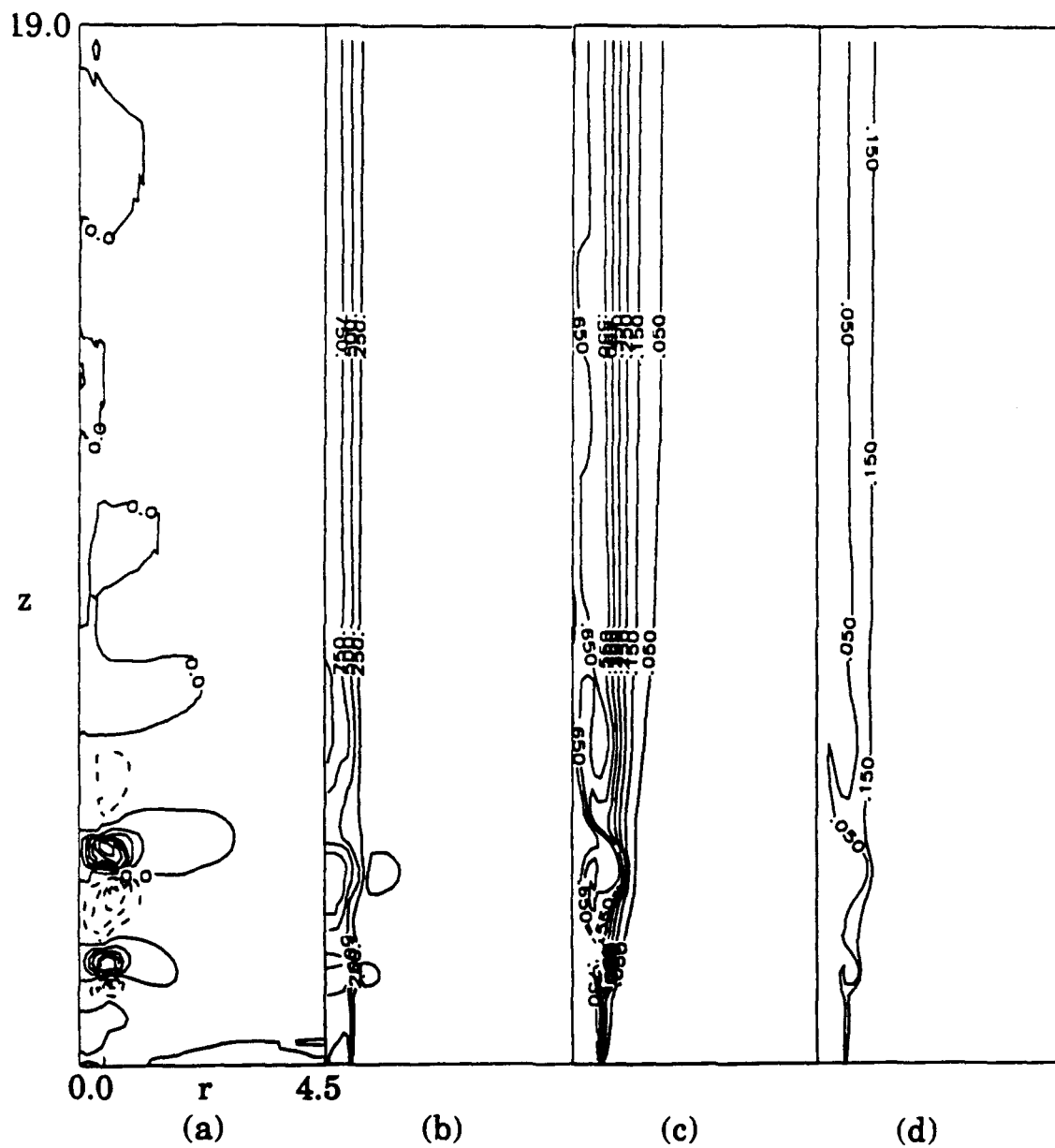


Figure 2. Contours of (a) radial velocity, (b) axial velocity, (c) mole fraction H_2 , (d) mole fraction O_2 for a nonreacting, zero-gravity jet of $H_2 - N_2$ into coflowing air. Dimensions are in cm, velocities are in cm/s.

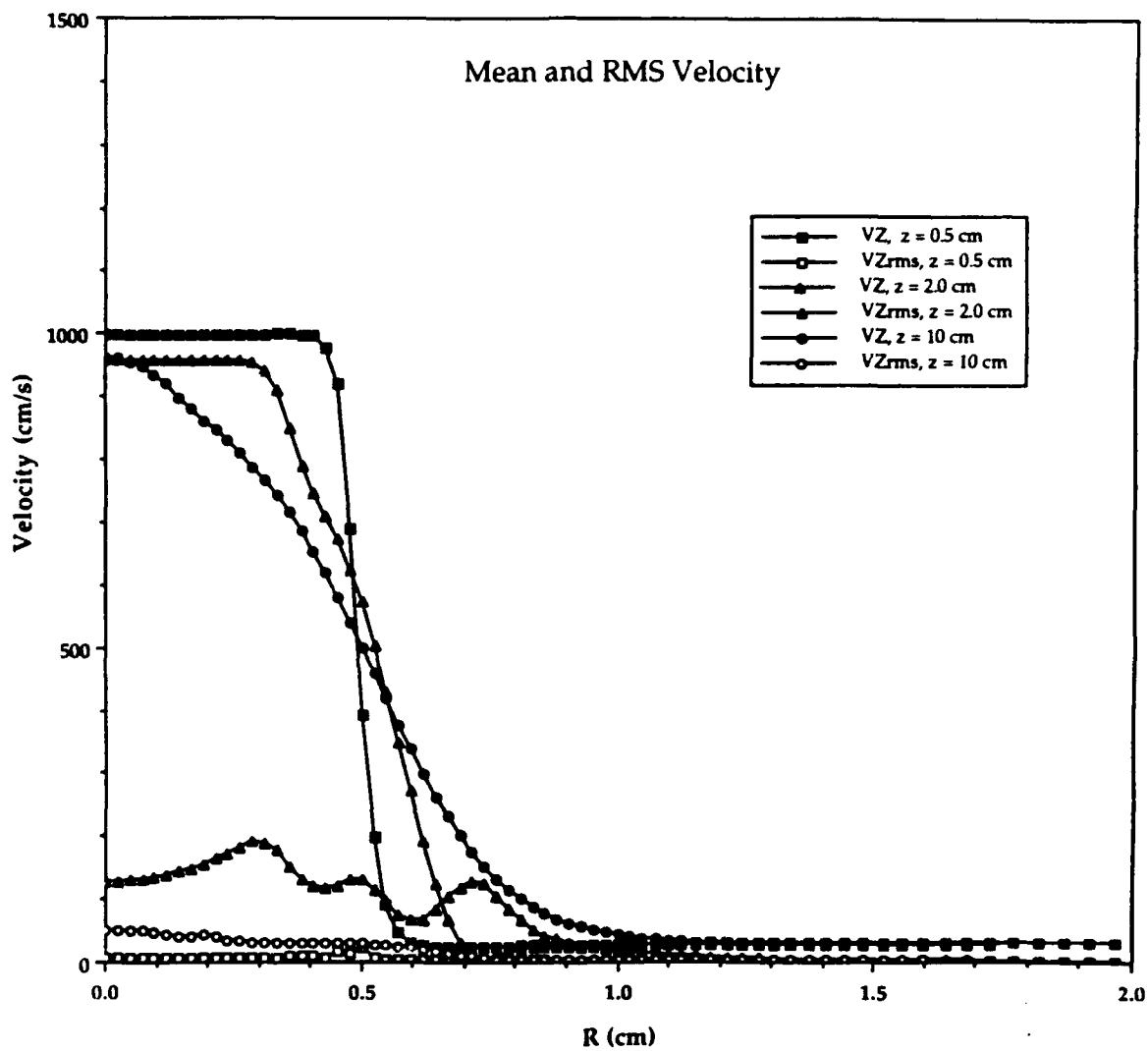


Figure 3. Mean and rms velocity for the zero-gravity nonreacting jet at three axial locations.

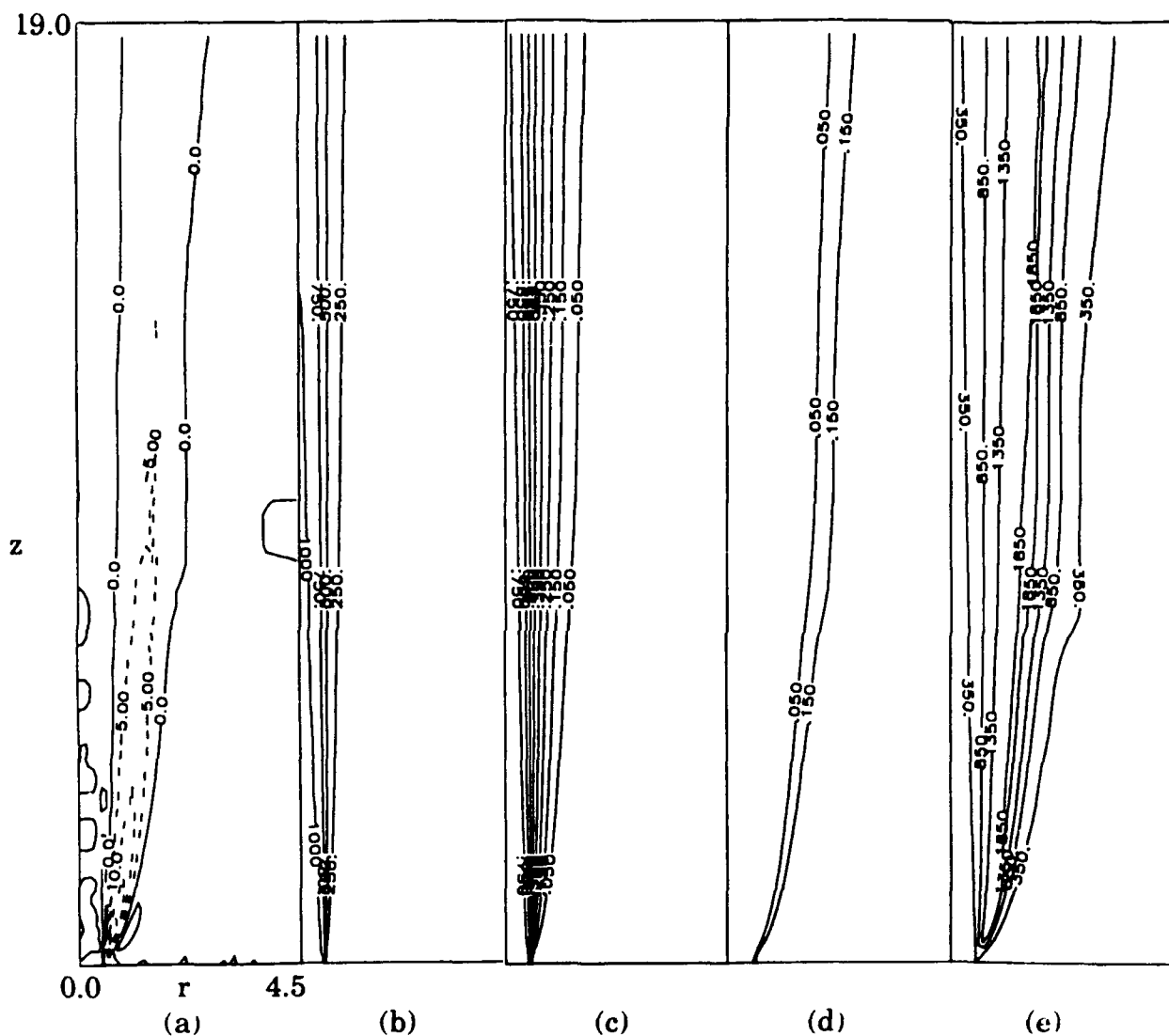


Figure 4. Contours of (a) radial velocity, (b) axial velocity, (c) mole fraction H_2 , (d) mole fraction O_2 , (e) temperature for a zero-gravity diffusion flame formed between a $H_2 - N_2$ jet and coflowing air. Dimensions are in cm, velocities are in cm/s, temperature is in K.

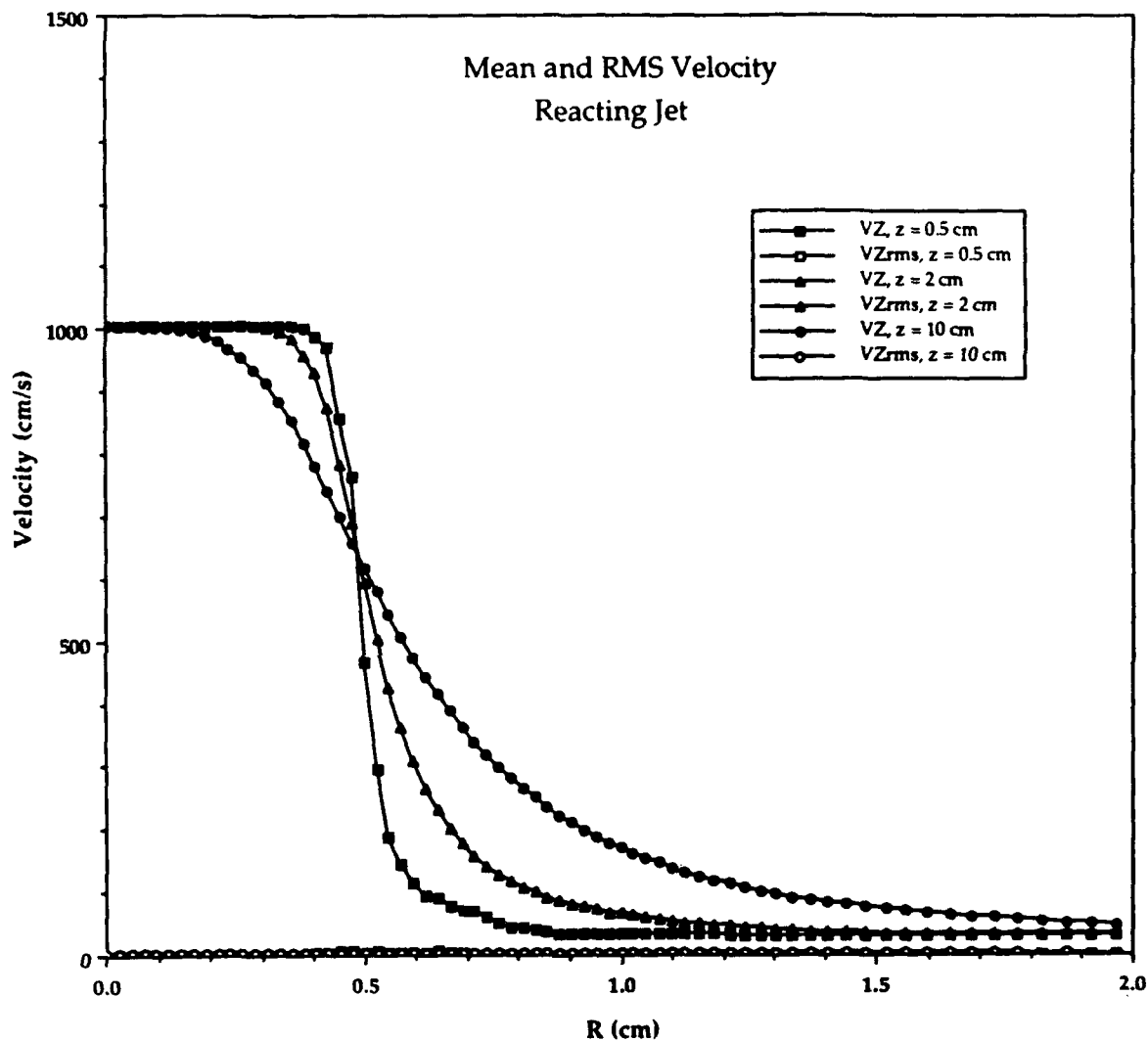


Figure 5. Mean and rms velocity for the zero-gravity diffusion flame at three axial locations.

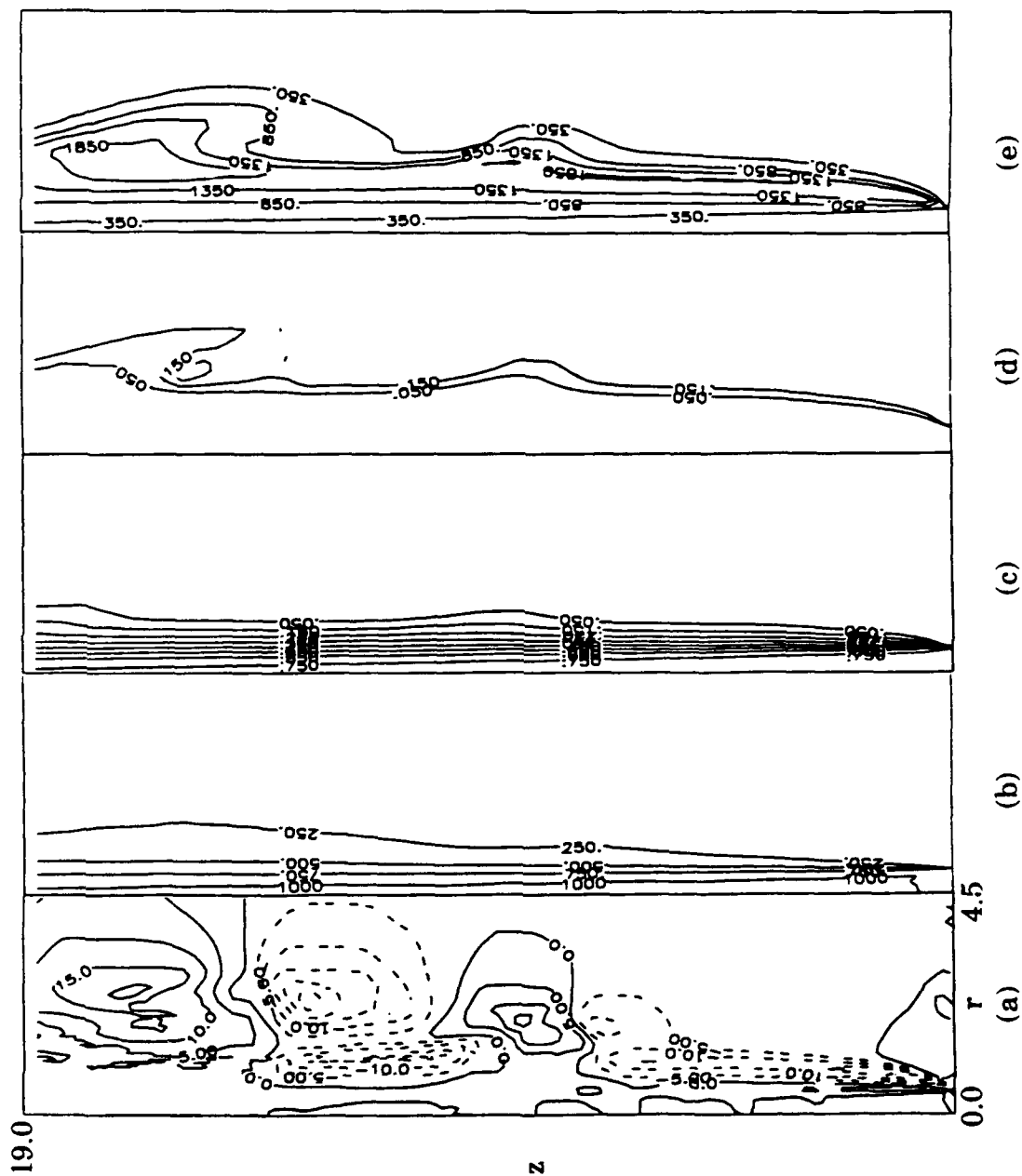


Figure 6. Contours of (a) radial velocity, (b) axial velocity, (c) mole fraction H_2 , (d) mole fraction O_2 , (e) temperature for normal-gravity diffusion flame formed between a $H_2 - N_2$ jet and coflowing air. Dimensions are in cm, velocities are in cm/s, temperature is in K.

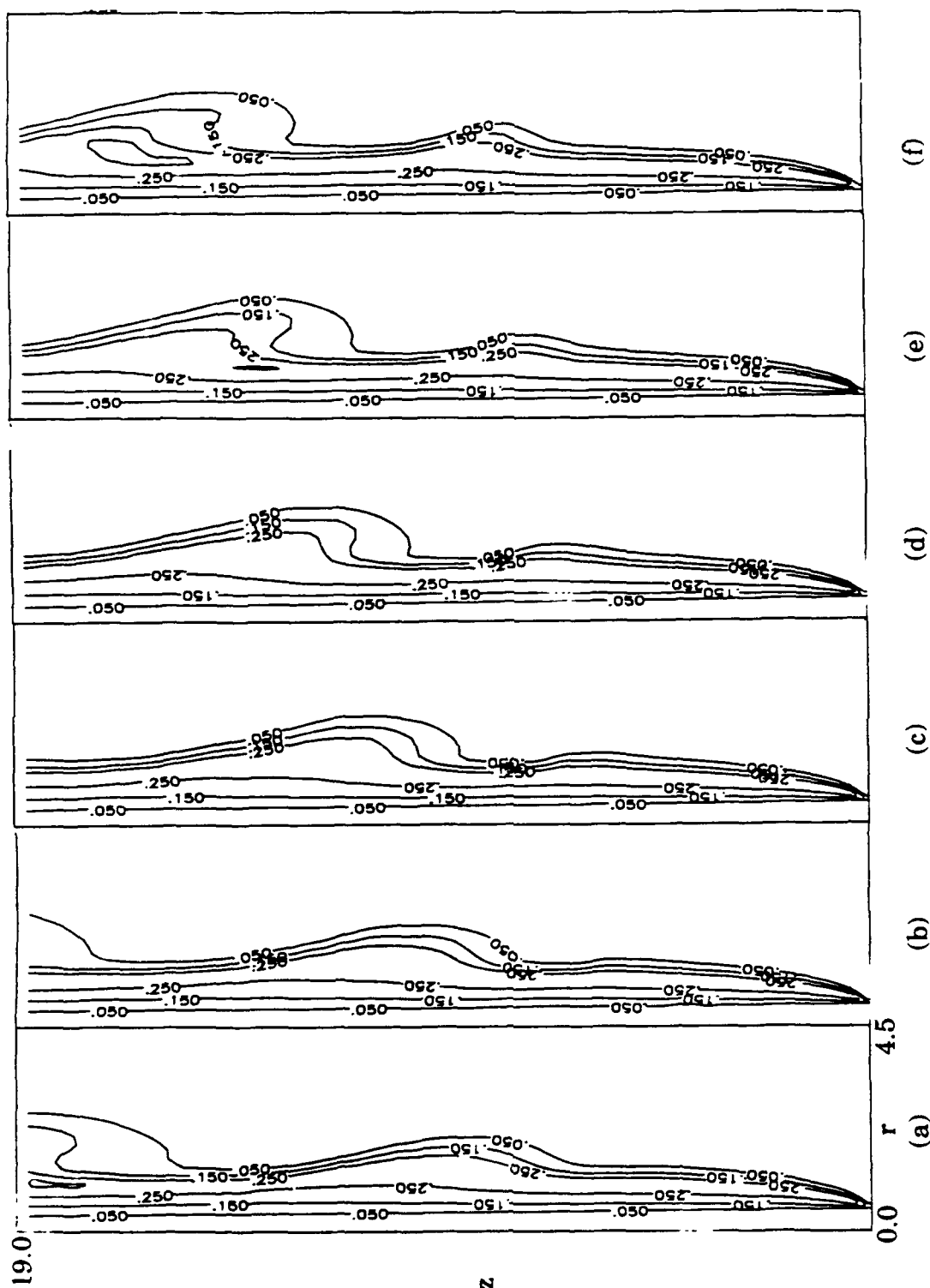


Figure 7. Sequence of contours of H_2O mole fraction showing the formation of the large vortical structures in the coflow region. The time interval between each frame is 11.25 ms.